



HOKKAIDO UNIVERSITY

| | |
|------------------|---|
| Title | ESTIMATION OF SURFACE ALBEDO FROM NOAA-AVHRR DATA |
| Author(s) | TANI, Hiroshi |
| Citation | Journal of the Faculty of Agriculture, Hokkaido University, 65(4), 331-341 |
| Issue Date | 1992-11 |
| Doc URL | https://hdl.handle.net/2115/13121 |
| Type | departmental bulletin paper |
| File Information | 65(4)_p331-341.pdf |



ESTIMATION OF SURFACE ALBEDO FROM NOAA-AVHRR DATA

Hiroshi TANI and Ikuo HORIGUCHI

Department of Agricultural Engineering,
Faculty of Agriculture, Hokkaido University,

Sapporo 060, Japan

(Received April 6, 1992)

Introduction

The ratio of reflected shortwave radiation to the corresponding incoming shortwave radiation (solar radiation), that is, the shortwave reflectivity of a surface, is referred to as its albedo. The albedo is the critical ground parameter determining the solar energy absorbed by the earth's surface, and it affects the earth's energy and water balance. Its distribution is therefore important for irrigation planning and estimation of water resources in agricultural areas.

Since radiance measured by satellites is directly related to surface reflectance values, satellite data are useful tools for deriving surface albedo maps. Some research has been done on estimation of albedo using satellite data from the climatological viewpoint. Data from satellites have been used to estimate surface albedo on various horizontal scales. Landsat was used for the distribution of surface albedo on a small scale (up to 10^2km)^{1,8)} and NOAA was used on a regional scale (to about 10^3km)^{4,5,9)}. In addition, a geostationary satellite was used to estimate albedo on a global scale^{10,11)}.

The objective of this study was to improve the method for the estimation of surface albedo over forests and cultivated land using data from the Advanced Very High Resolution Radiometer (AVHRR) onboard the TIROS-N/NOAA polar orbiter series of meteorological satellites.

When determining surface albedo, satellite data must be corrected for atmospheric effects such as scattering and absorption of solar radiation. In addition, narrow-to-broadband conversion must be performed in order to calculate total albedo from spectral albedos that are derived from satellite data. In this study, albedos were estimated by the use of two methods that differ in regard to atmospheric correction and narrow-to-broadband conversion. The estimation precision was examined by comparison with ground-truth data.

Methods

1. In situ measurements

The sites used in this study were the Tomakomai Experimental Forest, Hokkaido University (42°40'N, 141°36'E), a tillage area in Eniwa (42°56'N, 141°39'E) and pasture land in Abashiri (43°55'N, 144°23'E), located on the flat ground of a plateau (Tomakomai Experimental Forest) or a plain (tillage and pasture lands). The forest site was located in a relatively homogeneous deciduous forest, and the tillage and pasture sites comprised representative vegetation in their vicinities. We therefore assumed that the effect of spatial variability of surface albedo was small when relating ground observation data to NOAA-AVHRR's areal data (about 1 km²).

In situ data (surface albedo) were measured continuously at the three sites using pyranometers. In the forest and the pasture, two pyranometers (Neo Pyranometer manufactured by Eiko-Seiki Co., Ltd.) were installed at the same height above the vegetation but facing in opposite directions. Global solar radiation (downward flux) was observed by the pyranometer installed pointing upwards, and upward flux, radiation reflected by the vegetation, was observed by a pyranometer installed pointing downwards. An albedometer (manufactured by KIPP & ZONEN) consisting of two pyranometers for observation of surface albedo was used in the tillage area.

The pyranometer outputs were converted into 5-minute average values and recorded on floppy disks using digital data loggers (SOLAC III, manufactured by Eiko-Seiki Co., Ltd.) in the forest and the pasture, and 10-minute average values were recorded in the semiconductor memory by using a digital recorder (KADEC-UP, manufactured by KONA Systems Co., Ltd.) in the tillage area. While there was a difference in the average time at the sites, this can be ignored as changes in albedo are minimal during the NOAA overpass time (13 : 00-15 : 00). Observation was continuous from July 1 to October 22, 1990.

2. Deriving albedo from NOAA-AVHRR data

As a result of absorption and scattering by water vapor, ozone, and aerosols in the atmosphere, solar radiation is attenuated when passing through the atmosphere (Fig. 1). Consequently, the sensor of a satellite observes radiance affected by atmospheric absorption and scattering, and the value derived directly from satellite data is called planetary albedo. The planetary albedo is expressed as the ratio of the shortwave radiant flux density that goes out to space from the top of the atmosphere to the irradiance that goes into the atmosphere. Correction to convert planetary albedo into surface albedo, that is, atmospheric correction, is necessary.

The spectral intervals of AVHRR channel 1 (0.58-0.68 μm) and channel 2 (0.72-1.10 μm) are segments of the shortwave spectrum from 0.29 to 4.2 μm .

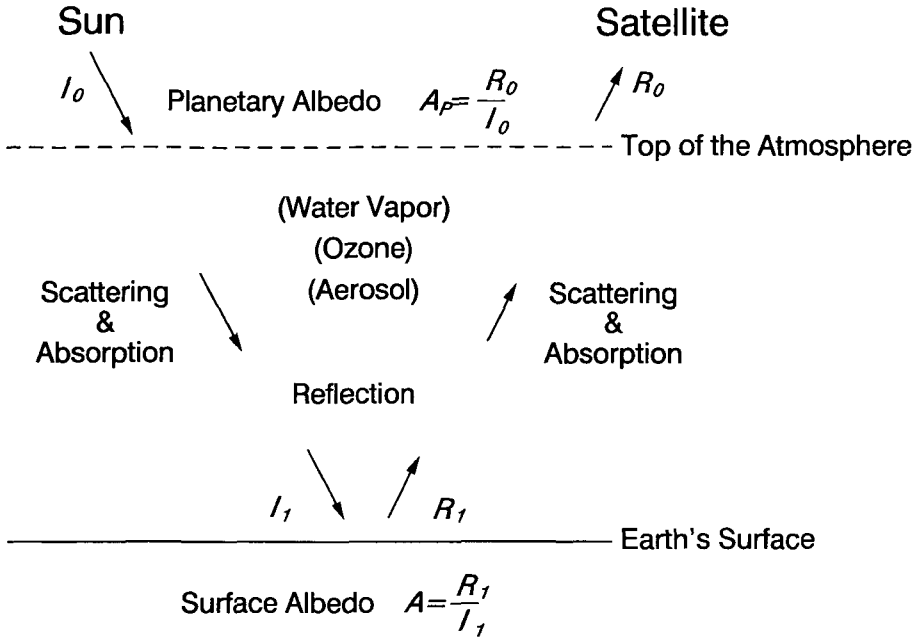


Fig. 1. Atmospheric effects on radiation transfer.

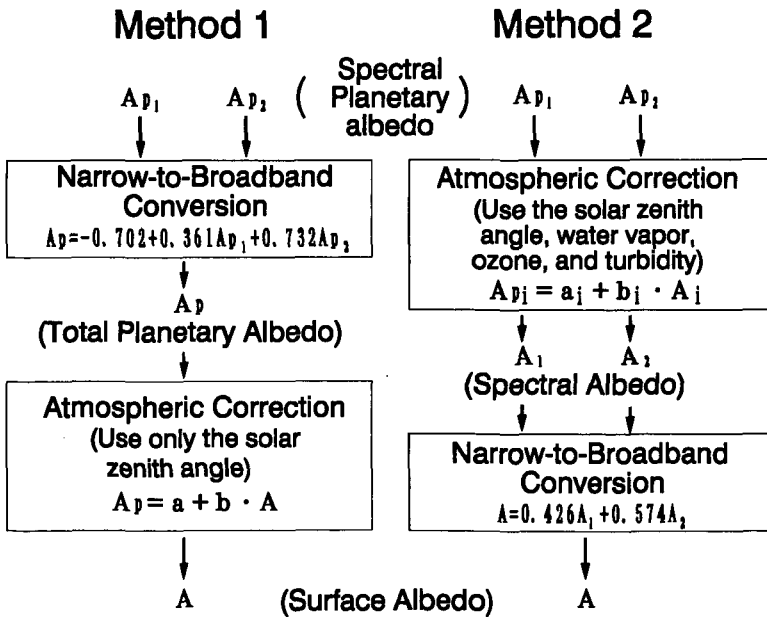


Fig. 2. Two methods for estimating surface albedo from NOAA-AVHRR data.

Therefore, it is necessary that the two narrowband quantities be converted to broadband quantities in order to derive total surface albedo (narrow-to-broadband conversion).

Two methods of estimating surface albedos using visible (channel 1) and near-infrared (channel 2) data from NOAA-AVHRR were examined in this study. The estimation procedures of the two methods are summarized in Fig. 2.

Assuming that the radiation field is isotropic, planetary albedo can be expressed as

$$A_{pi} = \frac{r_i}{\mu} \quad (1)$$

where A_{pi} is the planetary albedo of channel i , r_i is the reflectance factor of channel i , μ is the cosine of the solar zenith angle, and i denotes AVHRR channels 1 and 2. The reflectance factor to which AVHRR data counts are converted, by the use of a linear relationship¹²⁾, can be interpreted as the ratio of the irradiance of an isotropic radiation field with the measured radiance to solar irradiance.

The first method (Method 1) applies narrow-to-broadband conversion first. In this study a linear relationship for vegetated surfaces¹³⁾ was employed for narrow-to-broadband conversion, expressed as

$$A_p = -0.702 + 0.361 A_{p1} + 0.732 A_{p2} \quad (2)$$

where A_p is the planetary albedo of the total wavelength. This relationship was obtained from multivariate regression analysis of broadband data observed by Nimbus-7, and narrowband data observed by NOAA-7.

In order to derive the surface albedo from the planetary albedo, the latter should be corrected for atmospheric effects. In this study, a simple method²⁾ which suggests a linear relationship between clear-sky planetary and surface albedos for an aerosol-free atmosphere was used. The relationship is expressed as

$$A_p = a + bA \quad (3)$$

where a and b are coefficients dependent upon solar zenith angle, and A is the surface albedo.

With Method 2, which is an alternative approach to the estimation of albedo from NOAA-AVHRR data, spectral albedos are first calculated by atmospheric correction applied separately to visible (channel 1) and near-infrared (channel 2) data. We used a linear relationship between the planetary and surface albedos, in the same form as Eq. (3), as the atmospheric correction for both channels 1 and 2. This relationship is expressed as

$$A_{pi} = a_i + b_i A_i \quad (4)$$

where A_{pi} is the planetary albedo of channel i , A_i is the spectral albedo of channel

i , and a_i and b_i are coefficients for channel i . The coefficients were obtained by a numerical experiment that considered the effect of absorption, scattering and solar zenith angle⁷⁾. In order to use Eq. (4), these coefficients must be calculated from the radiosonde data, the ozone observation data and the Linke's turbidity factor obtained from direct solar radiation observation. In the present study these data were acquired at the Sapporo Meteorological Observatory (43°04'N, 141°20'E).

Surface albedo was then obtained by narrow-to-broadband conversion. For the narrow-to-broadband conversion, it is assumed that a surface albedo below a certain wavelength is equal to that of channel 1 and a surface albedo over that wavelength is equal to that of channel 2. Two spectral albedos are expressed as

$$A_1 = \frac{R_s}{I_s}, \quad A_2 = \frac{R_l}{I_l} \quad (5)$$

where R is the reflected solar radiation, I is the incident solar radiation, and subscript s and l denote shorter and longer wavelengths respectively. We set the border wavelength at $0.7 \mu\text{m}$, that is, the mid-wavelength between channels 1 and 2. Total albedo can be expressed by A_1 and A_2 as follows :

$$A = \frac{R_s + R_l}{I_s + I_l} = \frac{I_s}{I_s + I_l} A_1 + \frac{I_l}{I_s + I_l} A_2. \quad (6)$$

We can, therefore, compute the total surface albedo by a weighted average from the spectral albedos. The weighted values were determined by computing the spectral distribution of solar energy on the earth's surface using LOWTRAN6⁶⁾ which is radiation transfer model in the atmosphere. That is, radiant energy at the earth's surface on the shorter wavelength and the longer wavelength was computed by LOWTRAN6, and the fraction of the total radiant energy represented by each was calculated. In consequence, the narrow-to-broadband conversion by a weighted average is expressed as

$$A = 0.426 A_1 + 0.574 A_2. \quad (7)$$

NOAA-11 AVHRR full-scene images were used in this study. The satellite data were first processed by geometric correction using ground control points that were easy to identify on both the images and the maps. The correction errors at the control points were less than 1 pixel. Using site location information, digital count values of two channels for each of the three study sites were extracted from the corrected images. Surface albedos were then estimated by the two methods mentioned above.

Results and Discussion

The NOAA observation date, time, and the ground observation sites where in situ data were obtained are summarized in Table 1. We obtained a cloud-free data set for the ground observation sites by visual inspection of channel 1 images

Table 1. NOAA observation dates and times, and ground observation sites where NOAA-AVHRR cloud-free data were obtained. A hyphen indicates that the observation site in the image was obscured by cloud or that ground observation was missed.

| Observation date | Time | Ground observation site |
|------------------|---------|--------------------------|
| 1990. 5. 9 | 13 : 27 | - - pasture |
| 1990. 6.18 | 12 : 54 | - - pasture |
| 1990. 7. 1 | 12 : 13 | forest, tillage, pasture |
| 1990. 7. 2 | 13 : 42 | - tillage, pasture |
| 1990. 8. 2 | 13 : 05 | forest - - |
| 1990. 8. 3 | 12 : 54 | forest, tillage - |
| 1990. 8. 8 | 13 : 40 | forest, tillage - |
| 1990. 8.18 | 13 : 31 | - - pasture |
| 1990. 9. 8 | 13 : 02 | forest, tillage, pasture |
| 1990. 9.16 | 13 : 14 | - tillage, pasture |
| 1990. 9.21 | 12 : 20 | forest, - pasture |

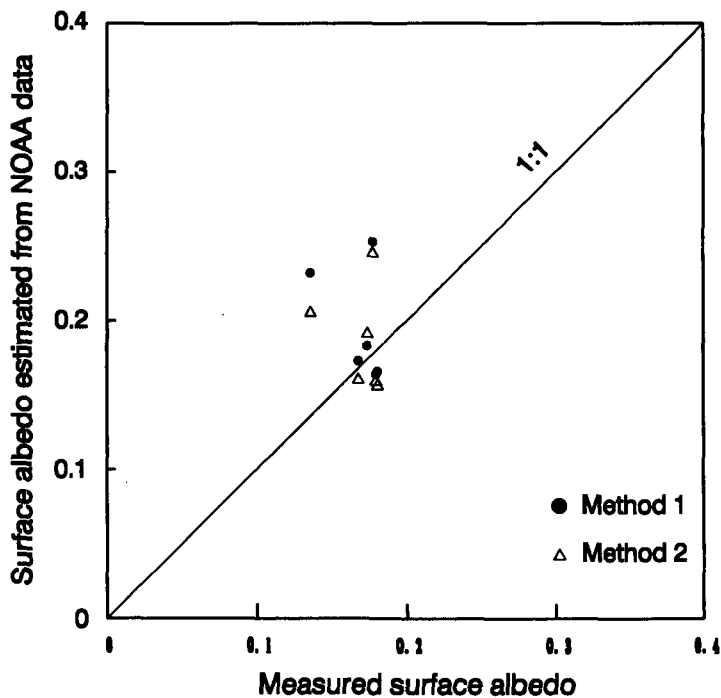


Fig. 3. Comparison between estimated albedos from NOAA data and measured albedos on tillage area.

from eleven acquired images. Finally, six coincident pairs of ground observation data and NOAA data were available for forest, six pairs for tillage, and eight pairs for pasture lands.

Comparison between ground-measured albedos and estimated albedos by the

use of the two methods are shown for tillage land in Fig. 3. While the albedos on two days (July 2 and August 8) were overestimated by both methods, the others are distributed near the 1 : 1 line. The same comparison of methods for pasture land is shown in Fig. 4. When estimated albedos are compared in detail, values estimated by Method 1 were always larger than those by Method 2.

The tendency for estimated albedos obtained by Method 1 to be larger than those obtained by Method 2 was also seen for the forest (Fig. 5). In addition, the estimated albedos for the forest by Method 2 are distributed closer to the 1 : 1 line than those estimated by Method 1.

The residuals (difference between estimated albedo and measured albedo) are shown in Table 2. Mean residuals and standard deviations of residuals obtained by Method 1 were larger than those by Method 2 for all sites. When a t-test of paired differences was performed, the difference between residuals in the two methods had a level of significance of 0.05 for the forest and the pasture. If all data are combined, the difference between the two methods has a level of significance of 0.01.

Comparing albedos estimated by NOAA with ground-measured albedos on three kinds of vegetation, we found that the estimated albedos tended to be too high, and this was particularly true for Method 1. The main difference between Method 1 and Method 2 is that Method 1 uses only the solar zenith angle for

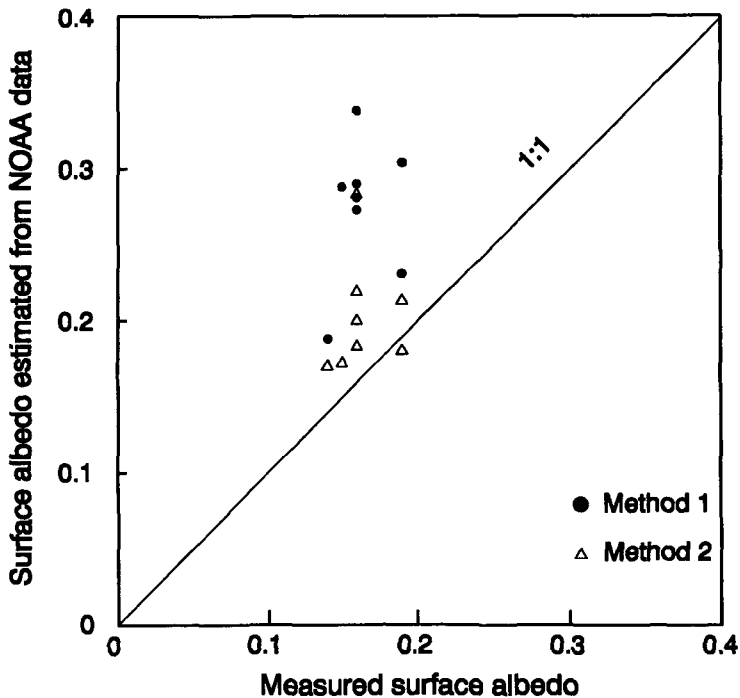


Fig. 4. Comparison between estimated albedos from NOAA data and measured albedos on pasture land.

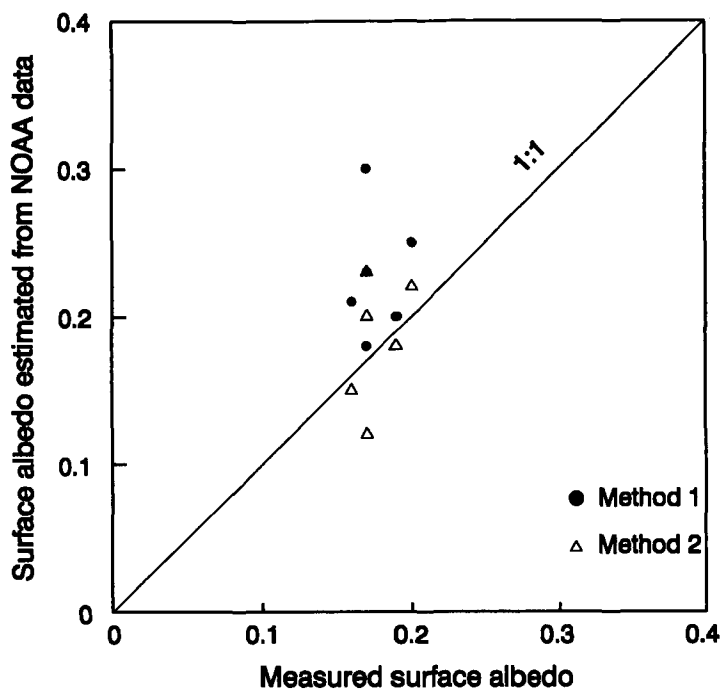


Fig. 5. Comparison between estimated albedos from NOAA data and measured albedos on forest.

Table 2. Mean and standard deviation of residuals of estimated albedo by two methods (upper : Method 1, lower : Method 2).

| Site | Mean residuals | Standard deviation | |
|--------------------|----------------|--------------------|--------|
| | | of residuals | Number |
| Forest (Tomakomai) | 0.052 | 0.037 | 6 |
| | 0.005 | 0.032 | 6 |
| Tillage (Eniwa) | 0.025 | 0.043 | 6 |
| | 0.016 | 0.038 | 6 |
| Pasture (Abashiri) | 0.110 | 0.042 | 8 |
| | 0.038 | 0.036 | 8 |
| Total | 0.067 | 0.055 | 20 |
| | 0.022 | 0.038 | 20 |

atmospheric correction, while Method 2 includes conditions and contents of the atmosphere that influence absorption and scattering of radiation, as well as the solar zenith angle. By Method 2, therefore, NOAA data were properly corrected for the state of the atmosphere at the time of the satellite observation. As a result, the superiority of Method 2 over Method 1 was shown by the above-mentioned statistical test.

Forest-site standard deviation of residuals was somewhat smaller than for the other two sites for both methods (Table 2). Spatial variability of albedo in

one pixel of NOAA data might effect this difference of dispersion. The effect of spatial variability of albedo was not so small for pasture and tillage lands, as assumed, when relating ground observation data to NOAA's areal data, and the magnitude of the effect was different among the three sites.

Estimated albedos by Method 2 are always larger than ground-measured albedos in the pasture, which is not the case for the other two sites. One of the reasons for this is that the Abashiri observation site is located 280 km from Sapporo, where the atmospheric parameters for atmospheric correction were obtained. According to a study of ground surface temperature estimation³⁾, the homogeneity of water vapor content distribution in the atmosphere cannot be guaranteed over a horizontal distance of only 77 km.

A comparison between the estimated albedos by NOAA and ground-measured albedos at all three sites is shown in Fig. 6. The range of estimated albedos is wider than that of ground-measured albedos. The main reason for this is that the reflection of solar radiation by vegetation surfaces was assumed to be isotropic in this study. But characteristics of reflection on actual vegetation vary with the sun-target-satellite geometry. In order to correct for this effect, problems of bidirectional reflectance distribution function and other related factors must be investigated.

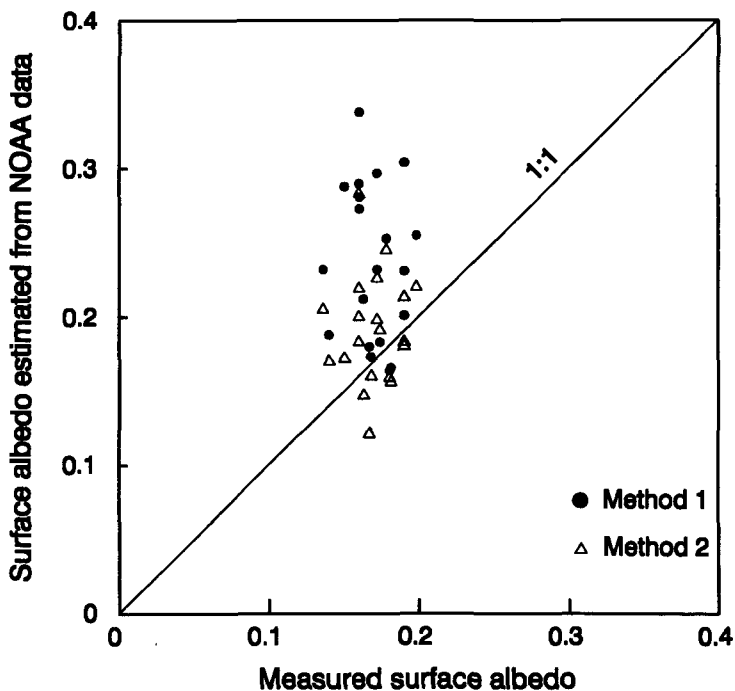


Fig. 6. Comparison between estimated albedos from NOAA data and measured albedos on the 3 observation sites.

Summary

Two methods for estimation of surface albedo using visible and near-infrared data from the Advanced Very High Resolution Radiometer (AVHRR) onboard NOAA-11 are examined. In Method 1, planetary albedo is derived by narrow-to-broadband conversion using empirical relationships, and then surface albedo is obtained by correction for the atmospheric attenuation effect. In Method 2, spectral albedos are calculated first by atmospheric correction applied to visible and near-infrared data, separately, and surface albedo is obtained by a weighted average narrow-to-broadband conversion.

The derived surface albedos are compared with those collected on several days coincident with NOAA overpass time for forest, tillage, and pasture sites in Hokkaido.

A comparison of the results by Method 1 and Method 2 indicates that the latter is superior to the former and may yield good estimates. The biases (satellite-minus-observed) of Method 1 and Method 2 are 0.067 and 0.022 respectively. Standard deviations of residuals are 0.055 and 0.038 for Method 1 and Method 2 respectively. Accordingly, atmospheric correction is best done for visible and near-infrared bands separately, as in Method 2. The main reason of the large standard deviation of residuals is the assumption that the radiation field is isotropic. In order to improve the accuracy, it is necessary to apply a bidirectional reflectance model to the estimated isotropic albedos.

Literature Cited

1. BREST, C. : Seasonal albedo of an urban/rural landscape from satellite observations. *J. Climate Appl. Meteor.*, **26**, 1169-1187, 1987.
2. CHEN, T. S. and G. OHRING : On the relationship between clear-sky planetary and surface albedos. *J. Atmos. Sci.*, **41**, 156-158, 1984.
3. COOPER, D. I. and G. ASRAR : Evaluating atmospheric correction models for retrieving surface temperatures from the AVHRR over a tallgrass prairie. *Remote Sens. Environ.*, **27**, 93-102, 1989.
4. GUTMAN, G. : A simple method for estimating monthly mean albedo of land surfaces from AVHRR data. *J. Appl. Meteor.*, **27**, 973-988, 1988.
5. GUTMAN, G. : Albedo of the U. S. Great Plains as determined from NOAA-9 AVHRR data. *J. Climate*, **2**, 608-617, 1989.
6. KNEYZYS F. X., E. P. SHETTLE, W. O. GALLERY, J. H. CHETWYND, Jr., L. W. ABREU, J. E. A. SELBY, R. W. FENN and R. A. McCLATCHEY : Atmospheric Transmittance/Radiances : Computer Code LOWTRAN6, AFGL-TR-83-0187, Air Force Geophysics Laboratory, 200 pp., 1980.
7. KOEPKE, P. : Removal of atmospheric effects from AVHRR albedo. *J. Appl. Meteor.*, **28**, 1341-1348, 1983.
8. MEKLER, Y. and J. H. JOSEPH : Direct determination of surface albedos from satellite imagery. *J. Climate Appl. Meteor.*, **22**, 530-536, 1983.
9. OTTERMAN, J. and C. J. TUCKER : Satellite measurements of surface albedo and temper-

- atures in semi-desert., *J. Climate Appl. Meteor.*, **24**, 228-235, 1985.
10. PINTY, B., G. SZEJWACH and J. STUM : Surface albedo over the Sahel from METEOSAT radiances., *J. Climate Appl. Meteor.*, **24**, 108-113, 1985.
 11. PINTY, B. and G. SZEJWACH : A new technique for inferring surface albedo from satellite observations. *J. Climate Appl. Meteor.*, **24**, 741-750, 1985.
 12. RAO, C. R. N. : Pre-launch Calibration of channels 1 and 2 of the Advanced Very High Resolution Radiometer. NOAA Tech. Rep. NESDIS 36, U. S. Dept. of Commerce, 66 pp., 1987.
 13. WYDICK, J. E., P. A. DAVIS and A. GRUBER : Estimation of broadband planetary albedo from operational narrowband satellite measurements. NOAA Technical report NESDIS 27, U. S. Dept. of Commerce, 32 pp., 1987.